

Methods of Micromechanics and Nanoindentation Applied to Heterogeneous Structural Materials

Jiří Němeček¹, Vlastimil Králík², Jaroslav Vondřejc³ & Jitka Němečková⁴

Abstract: This paper is devoted to the assessment of effective elastic properties on several typical structural composites with heterogeneous microstructure. Nanoindentation is utilized to measure intrinsic phase properties at the scale below one micron. Statistical approach and deconvolution methodology are applied. Based on nanoindentation data, micromechanical properties are up-scaled (homogenized) within the representative volume element (RVE) by means of an analytical method and numerical FFT-based scheme. Good correlation of the methods was found for the tested materials due to the close-to-isotropic nature of the composites in the RVE.

Keywords: Micromechanics, Nanoindentation, Heterogeneous materials, Homogenization, FFT

1. Introduction

Structural materials such as concrete, gypsum, plastics, wood and even metals are often characterized by a heterogeneous nature on different length scales (10^{-9} - 10^0 m). Traditionally, their mechanical properties are assessed from macroscopic tests that can only describe overall (averaged) properties like overall Young's modulus or strength. Nowadays, it is possible to access also lower material levels and assess small-scale properties of individual material components. An exclusive role in this micromechanical testing is played by nanoindentation [1]. This technique provides mechanical data for very small volumes (nm- μ m) and intrinsic material phase properties can be evaluated.

Wide theoretical background has also been laid in the field of micromechanics together with the development of classical composites. Micromechanical approaches are applied for matrix-inclusion problems to search for effective properties of the whole representative volume element (RVE) [2]. Although, the theoretical development in micromechanics is tremendous the knowledge of the material microstructure and its micromechanical properties is a key factor in obtaining relevant results.

In this paper, we deal with the micromechanical prediction of the effective elastic properties for several structural materials on a scale of several hundreds of micron. Simple analytical and more complex numerical approaches are utilized.

¹ doc. Ing. Jiří Němeček, Ph.D., ČVUT, Fakulta stavební, Thákurova 7/2077, 166 29 Praha 6, Czech Republic, jiri.nemecek@fsv.cvut.cz

² Ing. Vlastimil Králík, ČVUT, Fakulta stavební, Thákurova 7/2077, 166 29 Praha 6, Czech Republic, vlastimil.kralik@fsv.cvut.cz

³ Ing. Mgr. Jaroslav Vondřejc, ČVUT, Fakulta stavební, Thákurova 7/2077, 166 29 Praha 6, Czech Republic, jaroslav.vondrej@fsv.cvut.cz

⁴ Ing. Jitka Němečková, Ph.D., ČVUT, Fakulta stavební, Thákurova 7/2077, 166 29 Praha 6, Czech Republic, jitka.nemekova@fsv.cvut.cz

2. Nanoindentation and evaluation of micromechanical data

The principle of nanoindentation lies in bringing a very small tip to the surface of the material to make an imprint. In this study, three-sided pyramidal (Berkovich) diamond indenter was used. The depth of penetration is usually very small (several tens to hundreds of nm) to access individual material phases. The affected volume from which the mechanical response is measured can be estimated as $3\times$ the penetration depth. In our case the penetration depths were kept within 300 nm and thus, the affected volumes were below $1\ \mu\text{m}^3$. The loading history usually contains loading, holding and unloading periods. Standardly, elastic properties are evaluated for individual indents using analytical formulae, e.g. Oliver and Pharr methodology [3], which account for an elasto-plastic contact of a conical indenter with an isotropic half-space as:

$$E_r = \frac{1}{2\beta} \frac{\sqrt{\pi}}{\sqrt{A}} \frac{dP}{dh} \quad (1)$$

in which E_r is the reduced modulus measured in an experiment, A is the projected contact area of the indenter at the peak load, β is geometrical constant ($\beta=1.034$ for the used Berkovich tip) and dP/dh is a slope of the unloading branch evaluated at the peak. Elastic modulus E of the measured media can be found using contact mechanics which accounts for the effect of non-rigid indenter as:

$$\frac{1}{E_r} = \frac{(1-\nu^2)}{E} + \frac{(1-\nu_i^2)}{E_i} \quad (2)$$

in which ν is the Poisson's ratio of the tested material, E_i a ν_i are known elastic modulus and Poisson's ratio of the indenter.

For heterogeneous structural materials, the nanoindentation data are often measured in a large grid (Fig. 1) to cover the material heterogeneity. The distinction of the chemically and/or mechanically different material phases is often not possible on the microlevel ($<1\ \mu\text{m}$). It is, therefore, desirable to describe the material mechanical properties in a statistical sense. To assess individual phase properties, so called statistical deconvolution can be employed [4, 5]. In this method, experimental data are analyzed from the frequency plots. Mean elastic properties as well as phase volume fraction are estimated based on the best fit of the experimental data with a limited number of Gauss distributions (Fig. 3).

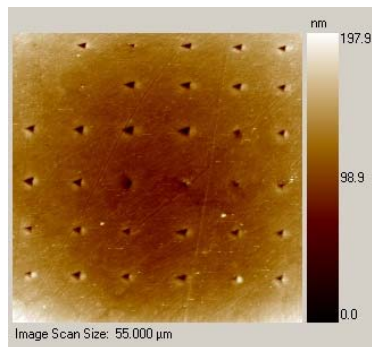


Fig. 1. AFM scan of indentation matrix on an aluminum alloy

3. Methods of micromechanics

In order to describe heterogeneous systems and their effective properties in a statistical sense, representative volume element (RVE) have been previously introduced [2]. RVE statistically represents a higher structural level of the material and serves for evaluation of the effective (homogenized) properties within the defined volume. It includes all microstructural inhomogeneities that should be substantially smaller than the RVE size.

Different assumptions on the geometry of inclusions, loading and boundary conditions can be utilized over the RVE to assess effective composite properties which leads to derivation of different analytical or numerical methods. RVE with substantially smaller dimensions than the macroscale body allows imposing homogeneous boundary conditions over the RVE. This leads to constant stress/strain fields in individual microscale components of ellipsoidal shapes [6]. Effective elastic properties are then obtained through averaging over the local contributions. Various estimates considering special choices of the reference medium known as rule of mixtures, Mori-Tanaka method or self-consistent scheme can be used [2]. For the case of composite material with prevailing matrix and spherical inclusions Mori-Tanaka method [7] was previously found to be simple but powerful tool to estimate effective composite properties also for structural materials and was used in this study.

Local strain and stress fields in RVE can also be found by numerical methods like finite element method or method based on Fast Fourier Transformation (FFT) [8,9]. The former one was proved to be reliable and computationally inexpensive method which only utilizes mechanical data in discretization (grid) points that perfectly match with the concept of nanoindentation. Therefore, the FFT method was chosen for our purposes.

3.1. Comparison of analytical and numerical schemes

Simple analytical methods (Mori-Tanaka) work with the assumption of isotropic effective properties. Such assumption is usually acceptable for the disordered structural materials. The comparison of an analytical and FFT schemes includes an assessment of the stiffness matrix (here in Mandel's notation) for isotropic material assuming plane strain conditions (equally with the FFT scheme) as:

$$\mathbf{L}_{\text{eff}}^{\text{A}} = \frac{E_{\text{eff}}}{(1 + \nu_{\text{eff}})(1 - 2\nu_{\text{eff}})} \begin{bmatrix} 1 - \nu_{\text{eff}} & \nu & 0 \\ \nu & 1 - \nu_{\text{eff}} & 0 \\ 0 & 0 & 1 - 2\nu_{\text{eff}} \end{bmatrix} \quad (3)$$

in which E_{eff} and ν_{eff} are effective Young's modulus and Poisson's ratio, respectively. The difference between the analytical and numerical stiffness matrices can be expressed using a stiffness error norm:

$$\delta = \sqrt{\frac{(\mathbf{L}_{\text{eff}}^{\text{FFT}} - \mathbf{L}_{\text{eff}}^{\text{A}}) :: (\mathbf{L}_{\text{eff}}^{\text{FFT}} - \mathbf{L}_{\text{eff}}^{\text{A}})}{(\mathbf{L}_{\text{eff}}^{\text{FFT}} :: \mathbf{L}_{\text{eff}}^{\text{FFT}})}} \quad (4)$$

in which $\mathbf{L}_{\text{eff}}^{\text{FFT}}$ is the effective stiffness matrix computed by the FFT method.

4. Materials

Several heterogeneous structural materials were selected for this study. Firstly, effective elastic properties were estimated for cement paste which is a basic component of a wide range of cementitious composites. Cement paste was prepared from Portland cement CEM-I 42,5 R (locality Mokra, CZ) with water to cement weight ratio equal to 0.5. Samples were stored in water for several years. Therefore, high degree of hydration can be anticipated in the samples.

The microstructure of cement paste includes several chemical phases, namely calcium-silica hydrates (C-S-H), calcium hydroxide $\text{Ca}(\text{OH})_2$, residual clinker, porosity and some other minor phases.

Secondly, dental gypsum (Interdent[®]) was chosen as a model representative for gypsum based materials. Samples were prepared with water to gypsum ratio 0.2. From the chemistry point of view, every gypsum binder is composed of three main components – calcium sulphate anhydrite (CaSO_4) in different modifications, calcium sulphate hemihydrate ($\text{CaSO}_4 \cdot \frac{1}{2}\text{H}_2\text{O}$) – α - or β -gypsum, and calcium sulphate dihydrate ($\text{CaSO}_4 \cdot 2\text{H}_2\text{O}$). The gypsum binder consists also some impurities and additives in case of natural sources. The Interdent gypsum is a low-porosity purified α -gypsum used for dental purposes.

Thirdly, an aluminium alloy was studied. The material consisted of aluminium intermixed with 1.5 wt.% of calcium and 1.6 wt.% TiH_2 . The material is used for the production of lightweight aluminium foams.

Microstructures of the selected materials are shown in Fig. 2. Dark areas can be attributed to the microporosity in the matrix whereas lighter areas belong to individual microstructural components. The images show on the heterogeneity of the samples in tested RVEs whose dimensions are $\sim 100\text{-}200\ \mu\text{m}$.

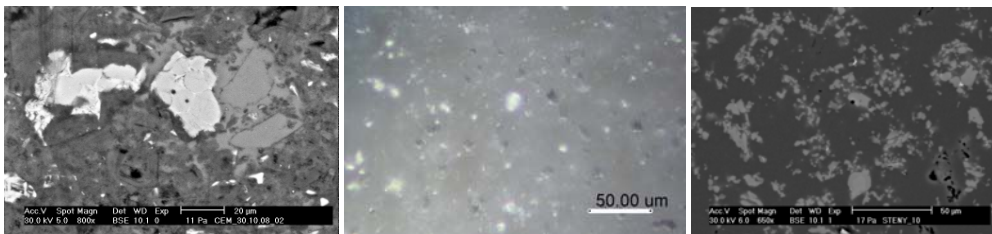


Fig. 2. Microstructures of cement paste (left), dental gypsum (mid) and aluminium alloy (right)

5. Results and discussion

Cement paste was indented by a grid consisting of $20 \times 20 = 400$ indents with $10\ \mu\text{m}$ spacing which yields the RVE size $\sim 200\ \mu\text{m}$. The resulting frequency plot of elastic moduli was deconvoluted into five mechanical phases as specified in Table 1. The phases correspond to the peaks showed in Fig. 3. They are denoted as A=low stiffness phase, B=low density C-S-H, C=high density C-S-H, D= $\text{Ca}(\text{OH})_2$, E=clinker. In this case, the notation of mechanically distinct phases matches well with the cement chemistry.

Nanoindentation data received from gypsum samples showed on crystalline nature of the composite with an anisotropic character. Two locations were tested. Each place was covered by $15 \times 12 = 180$ indents with $15\ \mu\text{m}$ spacing. The RVE size is then $\sim 200\ \mu\text{m}$. Since the gypsum crystals are dispersed in the sample volume in a random manner, surface measurements by nanoindentation show high scatter. However, several characteristic peaks can be distinguished in the frequency plots of elastic moduli and thus mechanically distinct phases separated. Three peaks (low stiffness, dominant and high stiffness phases) were identified (Fig. 3 and Table 2).

Two mechanically distinct phases were separated in the statistical deconvolution on Al-alloy sample. Results from 200 indents (two locations 10×10 indents) with $10\ \mu\text{m}$ spacing were evaluated. The RVE size is $\sim 100\ \mu\text{m}$ in this case. The dominant phase is denoted as Al-rich zone, whereas the lower stiffness phase is denoted as Ca/Ti-rich area in Fig. 3 and Table 3.

Based on the nanoindentation data after deconvolution analytical homogenization scheme (Mori-Tanaka) was employed for the assessment of effective RVE elastic properties. Resulting elastic properties of studied materials are shown in Tables 1-3.

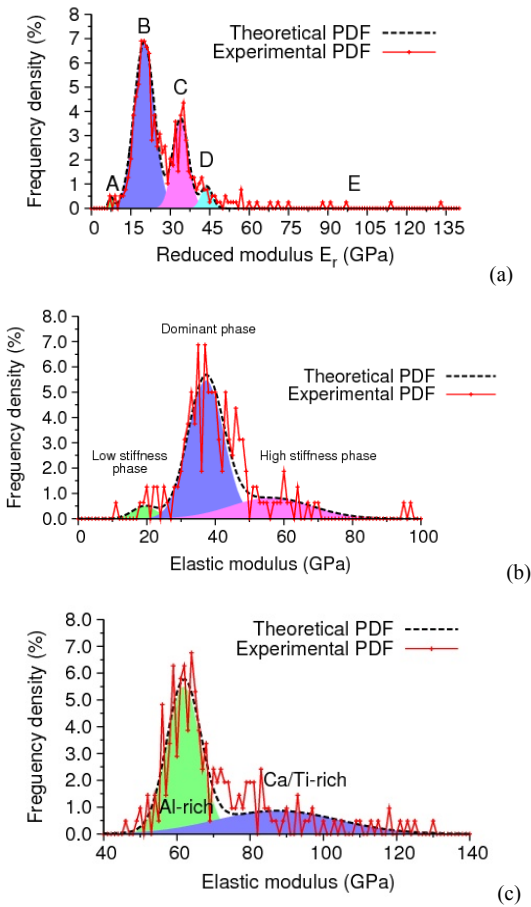


Fig. 3. Deconvolution of modulus of elasticity frequency plots into mechanical phases on (a) cement paste, (b) gypsum, (c) Al-alloy

Table 1. Data received from statistical deconvolution (input) and homogenized (output) values on cement paste.

	Phase	E (GPa)	Poisson's ratio (-)	Volume fraction
INPUT	Low stiffness	7.45	0.2	0.0105
	Low density C-S-H	20.09	0.2	0.6317
	High density C-S-H	33.93	0.2	0.2634
	Ca(OH) ₂	43.88	0.3	0.0461
	clinker	130	0.3	0.0483
OUTPUT	M-T homogenized value	25.3308	0.2067	1.0

Table 2. Data received from statistical deconvolution (input) and homogenized (output) values on gypsum.

	Phase	E (GPa)	Poisson's ratio (-)	Volume fraction
INPUT	Low stiffness	19.357	0.2	0.043750
	Dominant	37.234	0.2	0.712500
	High stiffness	56.277	0.2	0.243750
OUTPUT	M-T homogenized value	40.000	0.2	1.0

Table 3. Data received from statistical deconvolution (input) and homogenized (output) values on Al-alloy.

	Phase	E (GPa)	Poisson's ratio (-)	Volume fraction
INPUT	Al-rich zone	61.882	0.35	0.637681
	Ca/Ti-rich zone	87.395	0.35	0.362319
OUTPUT	M-T homogenized value	70.083	0.35	1.0

The comparison of stiffness matrices from analytical Mori-Tanaka scheme, i.e. using Equation (3), and from FFT homogenization are given in the following. Equation 5 contains results for cement paste, Equations 6 for gypsum and Equation 7 for Al-alloy. The stiffness values are given in GPa. Respective error norms are computed in Equation 8.

$$\text{cement: } \mathbf{L}_{\text{eff}}^{\text{A}} = \begin{bmatrix} 28.145 & 7.036 & 0 \\ 7.036 & 28.145 & 0 \\ 0 & 0 & 21.109 \end{bmatrix} \quad \mathbf{L}_{\text{eff}}^{\text{FFT}} = \begin{bmatrix} 26.177 & 6.778 & 0.068 \\ 6.778 & 26.224 & 0.014 \\ 0.068 & 0.014 & 19.818 \end{bmatrix} \quad (5)$$

$$\text{gypsum: } \mathbf{L}_{\text{eff}}^{\text{A}} = \begin{bmatrix} 44.444 & 11.111 & 0 \\ 11.111 & 44.444 & 0 \\ 0 & 0 & 33.333 \end{bmatrix} \quad \mathbf{L}_{\text{eff}}^{\text{FFT}} = \begin{bmatrix} 40.995 & 10.593 & -0.349 \\ 10.593 & 41.726 & -0.024 \\ -0.349 & -0.024 & 30.909 \end{bmatrix} \quad (6)$$

$$\text{Al-alloy: } \mathbf{L}_{\text{eff}}^{\text{A}} = \begin{bmatrix} 112.479 & 60.566 & 0 \\ 60.566 & 112.479 & 0 \\ 0 & 0 & 51.913 \end{bmatrix} \quad \mathbf{L}_{\text{eff}}^{\text{FFT}} = \begin{bmatrix} 117.130 & 62.741 & -0.163 \\ 62.741 & 117.106 & -0.143 \\ -0.163 & -0.143 & 54.313 \end{bmatrix} \quad (7)$$

$$\text{Errors: } ^{\text{cement}} \delta = 0.071045, \quad ^{\text{gypsum}} \delta = 0.075138, \quad ^{\text{Al-alloy}} \delta = 0.0393058 \quad (8)$$

It is clear from the above equations that both simple analytical and advanced FFT-based method give comparable results in our case. It is primarily due to the close-to-isotropic nature of the tested materials within the specified RVE. Even if the stiffness matrices computed by FFT scheme contain some non-zero off-axis terms, they are very small which confirms the previous statement. The best agreement of the methods was reached on Al-alloy (error<4%) which can be attributed to the fact that both material phases (Al-rich, and Ca/Ti-rich zones) are much more homogeneous compared to the phases that appear in cement paste or gypsum. But even in case of cement and gypsum the errors (7.1% and 7.5%) are still acceptable and show on good agreement of the results received from different methods.

6. Conclusions

It was proved in this study that nanoindentation can be used for the assessment of micromechanical parameters of intrinsic material constituents at the scale below one micron.

The use of statistical indentation gives access to both phase properties as well as volume fractions. Three typical structural materials (cement paste, gypsum and Al-alloy) with heterogeneous microstructures have been tested. Effective properties of their RVEs (100-200 μm) were successfully determined with analytical Mori-Tanaka scheme and numerical FFT-based method. The performance of both approaches was in good agreement for the tested materials. Derived stiffness matrices can be further used in standard computational procedures (e.g. finite element models).

Acknowledgment

Support of the Czech Science Foundation (GAČR 103/09/1748), Agency of the Czech Technical University in Prague (SGS10/135/OHK1/2T/11) and Ministry of Education of the Czech Republic (Research Plan MSM 6840770003) is gratefully acknowledged.

References

- [1] Fischer-Cripps A.C., *Nanoindentation*, (Springer Verlag, 2002). ISBN 0-387-95394-9.
- [2] Zaoui A., “Continuum Micromechanics: Survey”, *Journal of Engineering Mechanics*, **128** (8), pp.808-816 (2002), ISSN 0733-9399.
- [3] Oliver W. and Pharr G., “An improved technique for determining hardness and elastic modulus using load and displacement sensing indentation experiments”, *Journal of Materials Research*, **7** (6), pp.1564-1583 (1992), ISSN 0884-2914.
- [4] Constantinides G., Chandran K.R., Ulm F.-J., Vliet K.V., “Grid indentation analysis of composite microstructure and mechanics: Principles and validation”, *Materials Science and Engineering: A*, **430** (1-2), pp.189-202 (2006), ISSN 0921-5093.
- [5] Němeček J., Šmilauer V., Kopecký L., “Nanoindentation characteristics of alkali-activated aluminosilicate materials”, *Cement and Concrete Composites*, **33** (2), pp. 163-170 (2011), ISSN 0958-9465.
- [6] Eshelby J.D., “The determination of the elastic field of an ellipsoidal inclusion and related problem”, *Proc. Roy. Soc. London A*, **241**, pp. 376–396 (1957), ISSN 1471-2946.
- [7] Mori T. and Tanaka K., “Average stress in matrix and average elastic energy of materials with misfitting inclusions”, *Acta Metallurgica*, **21** (5), pp. 571-574, 1973, ISSN 1359-6454.
- [8] Moulinec H. and Suquet P., “A fast numerical method for computing the linear and nonlinear mechanical properties of composites”, *Comptes rendus de l'Académie des sciences. Série II, Mécanique, physique, chimie, astronomie*, **318** (11), pp.1417-1423 (1994), ISSN 0764-4450.
- [9] Zeman J., Vondřejc J., Novák J., Marek I., “Accelerating a FFT-based solver for numerical homogenization of periodic media by conjugate gradients”, *Journal of Computational Physics*, **229** (21), pp. 8065-8071 (2010), ISSN 0021-9991.

